Actin Reorganization Triggers Rapid Cell Elongation in Roots[1]

Hirotomo Takatsuka,[a] Takumi Higaki,[b] and Masaaki Umeda[a,2,3]

[a]Graduate School of Science and Technology, Nara Institute of Science and Technology, Ikoma, Nara 630-0192, Japan

[b]International Research Organization for Advanced Science and Technology, Kumamoto University, Kumamoto 860-8555, Japan

ORCID ID: 0000-0003-3934-7936 (M.U.)

Root growth is controlled by mechanisms underlying cell division and cell elongation, which respond to various internal and external factors. In Arabidopsis (*Arabidopsis thaliana*), cells produced in the proximal meristem (PM) elongate and differentiate in the transition zone (TZ) and the elongation/differentiation zone (EDZ). Previous studies have demonstrated that endoreplication is involved in root cell elongation; however, the manner by which cells increase in length by more than 2-fold remains unknown. Here, we show that epidermal and cortical cells in Arabidopsis roots undergo two modes of rapid cell elongation: the first rapid cell elongation occurs at the border of the proximal meristem and the TZ, and the second mode occurs during the transition from the TZ to the EDZ. Our previous study showed that cytokinin signaling promotes endoreplication, which triggers the first rapid cell elongation. Our cytological and genetic data revealed that the second rapid cell elongation involves dynamic actin reorganization independent of endoreplication. Cytokinins promote actin bundling and the resultant second rapid cell elongation through activating the signaling pathway involving the cytokinin receptors ARABIDOPSIS HISTIDINE KINASE3 (AHK3) and AHK4 and the B-type transcription factor ARABIDOPSIS RESPONSE REGULATOR2. Our results suggest that cytokinins promote the two modes of rapid cell elongation by controlling distinct cellular events: endoreplication and actin reorganization.

Continuous root growth is achieved by sustainable cell division and subsequent cell elongation. In Arabidopsis (*Arabidopsis thaliana*), roots are divided into four distinct zones along the apical-basal axis: the stem cell niche, the proximal meristem (PM), the transition zone (TZ), and the elongation/differentiation zone (EDZ; Verbelen et al., 2006; Baluška et al., 2010; Takatsuka and Umeda, 2014). Stem cells surrounding the quiescent center give rise to daughter cells that divide multiple times in the PM. Upon cessation of cell division, cells start to differentiate and elongate in the TZ. After leaving the TZ, cells elongate more rapidly and are fully differentiated. Defective cell division in the PM or impaired cell elongation in the EDZ retards root growth, indicating that both cell division and cell elongation are indispensable for continuous root growth (Doerner et al., 1996; Takatsuka et al., 2009; Nowack et al., 2012; Haruta et al., 2014).

In plants, cell elongation occurs through multiple cellular processes, such as vacuole expansion, microtubule (MT) reorganization, and cell wall loosening (Rojo et al., 2001; Le et al., 2005; Verbelen et al., 2006). Dynamic regulation of F-actin, which is made from monomeric globular actin (G-actin), also plays an important role in the elongation of various types of cells. For example, disorganization of actin filaments causes defects in trichome development, lobe extension in pavement cells, and stomatal movement (Mathur et al., 1999; Szymanski et al., 1999; Fu et al., 2002, 2005; Higaki et al., 2010; Zhao et al., 2011). How cell elongation occurs in the EDZ and if actin reorganization is associated with controlling cell elongation in the root remain elusive.

Phytohormones play an essential role in regulating continuous root growth. Auxin promotes cell division and represses cell differentiation; the auxin gradient generated by the auxin transport facilitator PIN-FORMED (PIN) is critical for controlling cell division and, thereby, preserves the root meristem (Blilou et al., 2005). On the other hand, cytokinins (CKs) have an opposite function; namely, CKs repress cell division and promote cell differentiation in the roots. CK signaling is mediated by the two-component system, in which three ARABIDOPSIS HISTIDINE KINASEs, AHK2, AHK3, and AHK4, act as transmembrane receptors (Hwang and Sheen, 2001; Inoue et al., 2001; To and Kie-

[1]This work was supported by MEXT KAKENHI (Grant numbers 17H03965, 17H06477) to M.U., MEXT KAKENHI (Grant number 17K15415) and the 2017 Inamori Research Grant Program to H.T., and MEXT KAKENHI (Grant number 17K19380), a Grant for Basic Science Research Projects from The Sumitomo Foundation (160146), and The Canon Foundation to T.H.

[2]Author for contact: mumeda@bs.naist.jp.

[3]Senior author.

The author responsible for distribution of materials integral to the findings presented in this article in accordance with the policy described in the Instructions for Authors (www.plantphysiol.org) is: Masaaki Umeda (mumeda@bs.naist.jp).

M.U. and H.T. conceived the original research plans and wrote the article with contributions of all the authors; M.U. supervised the experiments; H.T. performed most of the experiments; T.H. provided technical assistance to H.T.; H.T. designed the experiments and analyzed the data.

www.plantphysiol.org/cgi/doi/10.1104/pp.18.00557

ber, 2008). After perceiving CK, the signal is cascaded through a phosphorelay to transcription factors named the B-type ARABIDOPSIS RESPONSE REGULATORs (ARRs) that, in turn, regulate the expression of a variety of CK-responsive genes (Sakai et al., 2001; To et al., 2004; Mason et al., 2005; To and Kieber, 2008). The B-type ARRs (*ARR1*, *ARR2*, and *ARR12*) are expressed locally in the TZ, and CK signaling is activated around this zone and promotes cell differentiation (Dello Ioio et al., 2007; Takahashi et al., 2013).

Dello Ioio et al. (2008) demonstrated that ARR1 and ARR12 directly induce the expression of *SHORT HYPOCOTYL2* (*SHY2*)*/INDOLE-3-ACETIC ACID INDUCIBLE3*, encoding a member of the auxin/indole-3-acetic acid (Aux/IAA) family of auxin signaling repressors, which then represses the expression of *PIN* and perturbs auxin flow, thereby inhibiting cell division and facilitating cell elongation to enter the TZ. Another role for CK is to promote the onset of endoreplication, a specialized mode of the cell cycle in which DNA synthesis (S phase) is repeated without mitosis or cytokinesis (Lee et al., 2009; Takahashi et al., 2013). Once the cells start endoreplication, their volume increases and they do not resume cell division; therefore, the onset of endoreplication defines the meristem size (Hayashi et al., 2013; Takahashi et al., 2013). We previously reported that CK-activated ARR2 induces the expression of *CELL CYCLE SWITCH52A1* (*CCS52A1*), which encodes an activator of the E3 ubiquitin ligase, anaphase-promoting complex/cyclosome (APC/C; Cebolla et al., 1999; Larson-Rabin et al., 2009). The CCS52A1-activated APC/C is involved in the degradation of mitotic cyclins, thereby inhibiting G2/M progression and triggering endoreplication. ARR2 also inhibits auxin signaling by up-regulating *SHY2* (Takahashi et al., 2013).

Here, we report that Arabidopsis root cells undergo two modes of cell elongation: the first is dependent of endoreplication, and the second requires actin rearrangement. CKs promote not only the onset of endoreplication but also actin bundling, indicating that CKs play a pivotal role in root cell elongation.

RESULTS

Two Modes of Cell Elongation in Arabidopsis Roots

To precisely describe the mode of cell elongation in Arabidopsis roots, we examined the cortical cell file. Measurement of cell length showed that the cortical cells underwent two steps of cell elongation. The first rapid cell elongation occurred when PM cells expanded and entered the TZ (Fig. 1, A and B; Verbelen et al., 2006; Takatsuka and Umeda, 2014). According to the conventional way, we defined the number of PM cells as those between the cortex/endodermis initial and the first TZ cell (Casamitjana-Martínez et al., 2003; Dello Ioio et al., 2007). In the TZ, cells elongated gradually but then displayed rapid elongation by about a 2-fold difference when compared with two neighboring cells in length (Fig. 1, A and B). A similar pattern of cell elongation was observed in every root used for measurement, although the timing of the onset of cell elongation varied between samples (Supplemental Fig. S1). We defined any cell longer than 1.5-fold of the neighboring shorter cell as the first EDZ cell. These two modes of cell elongation also were observed in the epidermis; both the trichoblast and atrichoblast cells also underwent a similar two-step cell elongation, although the timing of rapid cell elongation was different between the two cell files (Supplemental Fig. S2).

We reported previously that the first rapid cell elongation at the boundary between the PM and the TZ is triggered by endoreplication (Adachi et al., 2011; Takahashi et al., 2013; Takatsuka and Umeda, 2014, 2015). To examine whether the second rapid cell elongation also is associated with endoreplication, we monitored the incorporation of 5-ethynyl-2-deoxyuridine (EdU) during the progression of the S phase. Consistent with previous reports, frequent EdU incorporation was detected in cells just prior to or after entering the TZ, implying that DNA is replicated in both mitotic and endoreplicating cells (Fig. 1, C and D; Hayashi et al., 2013; Otero et al., 2016). By contrast, EdU incorporation was observed rarely in the last TZ or the first EDZ cells, suggesting that endoreplication ceases within the TZ and that the second rapid cell elongation is not triggered by endoreplication (Fig. 1, C and D). To support this idea, we used the *ccs52a1* mutant with an impairment in the onset of endoreplication and found that the number of PM cells, but not TZ cells, was increased (Fig. 1, E and F).

Neither Vacuole Dynamics Nor MT Rearrangement Is Associated with the Second Rapid Cell Elongation

In plants, cell elongation occurs through various intracellular events, such as cytoskeleton rearrangement and vacuole expansion. To know which event is associated with the second rapid cell elongation, we first studied vacuole dynamics by using transgenic plants expressing GFP fused to VACUOLAR MORPHOLOGY3 (VAM3), which is localized to the tonoplast membrane (Uemura et al., 2010). As shown in Supplemental Figure S3A, both the last TZ and the first EDZ cells contained large vacuoles. For the quantification of vacuole volume, we stained roots with 2′,7′-bis-(2-carboxyethyl)-5-(and-6)-carboxyfluorescein, acetoxymethyl ester (BCECF-AM). Then, we calculated the vacuole occupancy, the ratio of the vacuole volume to the total cell volume, and found that it increased gradually over the boundary between the TZ and the EDZ and never showed a sudden increase, even when more than 1.5-fold cell elongation occurred at the transition to the first EDZ cell (Supplemental Fig. S3, B and C). This suggests that vacuole expansion is unlikely to be a primary cause of the second rapid cell elongation.

We then examined MT rearrangement, a critical determinant of cell shape in plants (Dolan and Davies, 2004;

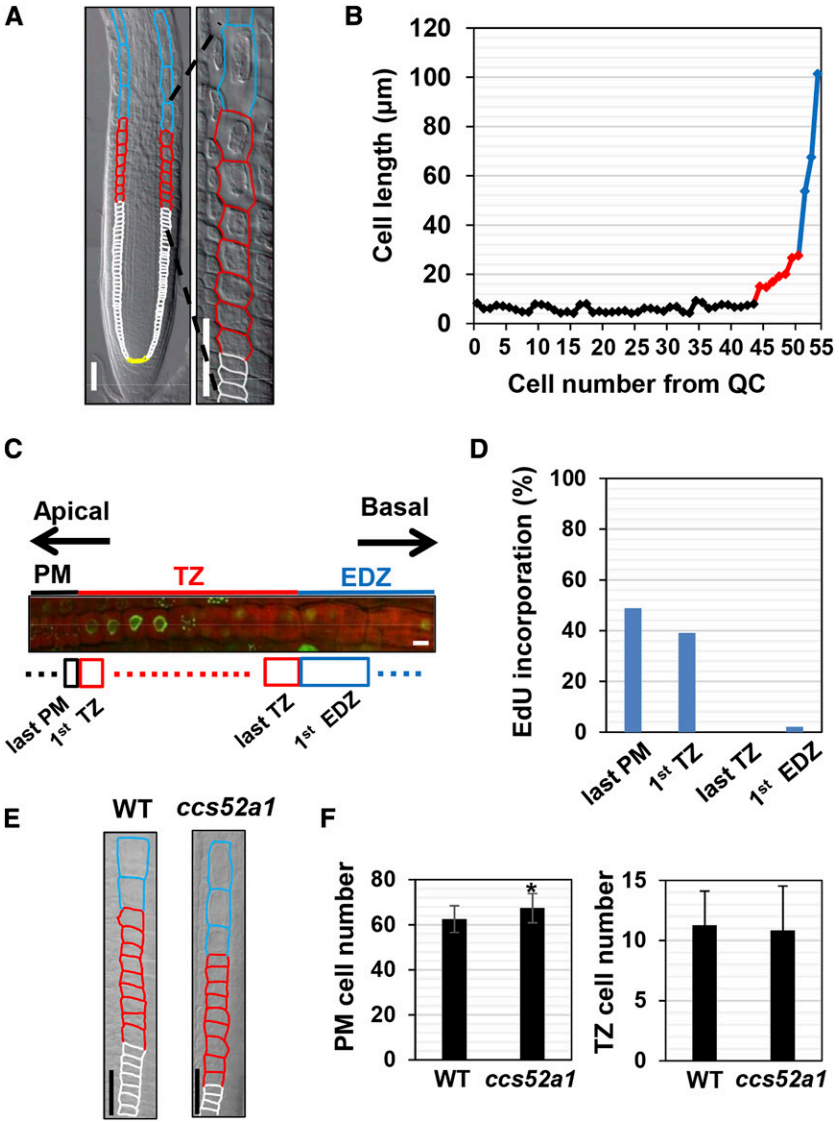

Figure 1. Two modes of rapid cell elongation in Arabidopsis roots. A, Distinct zones in the Arabidopsis root. Yellow, white, red, and blue outlines indicate cortical cells in the stem cell niche, the PM, the TZ, and the EDZ, respectively. A magnified image around the TZ is shown on the right. Bars = 50 μm. B, Cell length over the distinct zones of roots. Cortical cells were measured for cell numbers from the quiescent center (QC) and cell length. C, EdU incorporation around the TZ. Five-day-old roots were stained with EdU, and the cortical cell file was visualized by propidium iodide (PI) staining. Bar = 10 μm. D, Frequency of EdU incorporation into cortical cells. EdU signals were observed for the last PM cell, the first TZ cell, the last TZ cell, and the first EDZ cell. $n > 41$. E, Cortical cells around the TZ of 5-d-old wild-type (WT) and *ccs52a1* roots. Bars = 50 μm. F, Cell number in the PM and the TZ of wild-type and *ccs52a1* roots. Data are presented as means ± SD ($n > 24$). Significant differences from the wild type were determined by Student's *t* test: *, $P < 0.01$.

Braidwood et al., 2014). Immunostaining with the anti-tubulin antibody revealed that, in all tested samples ($n > 30$), MT organization was similar between the last TZ and the first EDZ cells (Supplemental Fig. S4A). To quantify the MT dynamics during the transition from the TZ to the EDZ, we determined two parameters: mean angle and parallelness (Higaki, 2017). This mean angle has the highest value of 90° when MTs have a complete transverse orientation and has the lowest value of 0° when MTs have a perfect longitudinal orientation. In addition, we also measured the MT parallelness, which indicates variations of MT orientations (Higaki, 2017). The parallelness can range from 0 to 1 and becomes higher as the MTs run parallel to each other. We found that both mean angle and parallelness did not change dramatically over the TZ and the EDZ (Supplemental Fig. S4B), suggesting that MT organization is stable during the second rapid cell elongation. To further investigate the role of MTs in the second rapid cell elongation, we treated wild-type roots with colchicine, an inhibitor of tubulin polymerization (Skoufias and Wilson, 1992). We calculated the MT occupancy, an indicator of the amount of cytoskeleton per unit of area (Higaki, 2017). The result showed that treatment with 10 or 50 μM colchicine significantly decreased the MT occupancy, indicating MT destabilization (Supplemental Fig. S4C). The same colchicine treatment reduced the cell number in the PM but not in the TZ (Supplemental Fig. S4, D and E). When treated with a higher concentration (200 μM) of colchicine, the severity of morphological abnormalities varied between individuals; cells in the EDZ were sometimes swollen abnormally (Baskin et al., 2004), making it difficult to conduct quantitative analysis. However, the boundary between the TZ and the EDZ still was apparent in the roots with a mild phenotype (Supplemental Fig. S4F). Taken together, our results suggest that MT rearrangement also is not the primary determinant of the second rapid cell elongation.

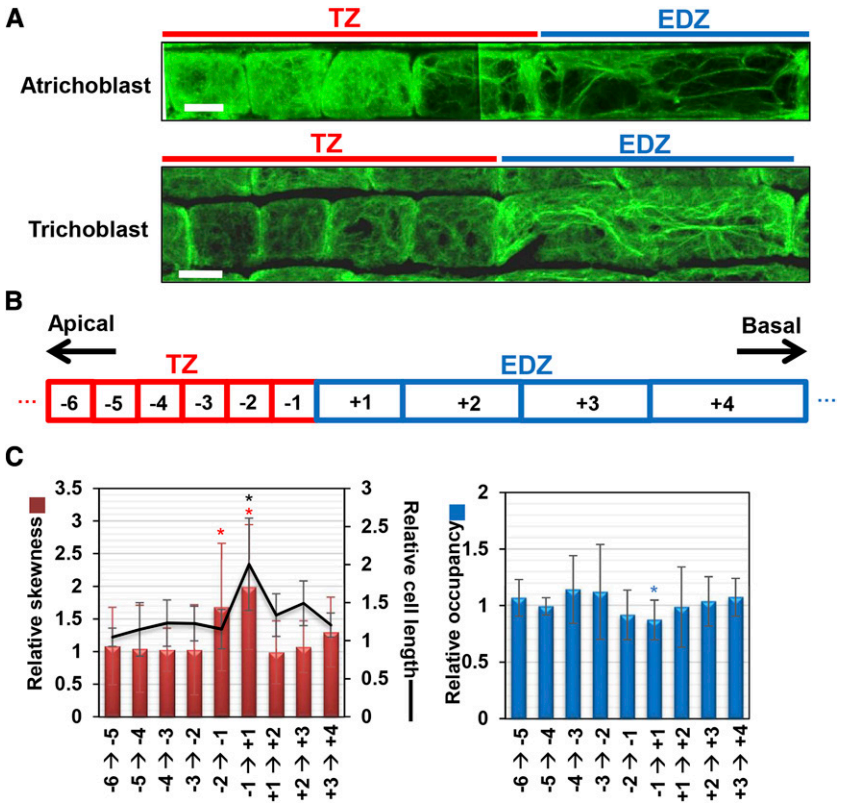

Figure 2. Actin reorganization at the boundary between the TZ and the EDZ. A, Actin filaments in atrichoblast and trichoblast cells at the boundary between the TZ and the EDZ. Immunostaining was conducted using the anti-actin antibody. Images were assembled from several photographs of different portions of roots. Bars = 10 μm. B, Diagram of epidermal cells at the boundary between the TZ and the EDZ. The numbers in the boxes indicate the positions of cells. C, Cell length, skewness, and occupancy of actin filaments at the boundary between the TZ and the EDZ. Each factor is indicated as a relative value, with that for the adjoining lower cell set to 1. Data are presented as means ± SD ($n > 30$). Significant differences from the adjoining lower cells were determined by Student's t test: *, $P < 0.05$. Red, blue, and black asterisks indicate significant differences for relative skewness, relative occupancy, and relative cell length, respectively.

Actin Reorganization Is Involved in the Second Rapid Cell Elongation

Actin plays an important role in cell elongation during root hair development, pollen tube growth, and trichome development (Smith and Oppenheimer, 2005; Pei et al., 2012; Fu, 2015). Therefore, we questioned if actin reorganization is associated with the second rapid cell elongation. Immunostaining with the anti-actin antibody showed that, in both atrichoblast and trichoblast cells of the epidermis, fine actin filaments were dispersed uniformly in the TZ (Fig. 2A). However, in the last TZ cell, longitudinally oriented actin bundles were apparent (Fig. 2A). To quantitatively evaluate actin filament bundling and density, we determined the skewness of intensity distribution and occupancy as a metric (Higaki et al., 2010; see "Materials and Methods"). Skewness indicates the degree of biased distribution of actin bundles in a cell. Occupancy represents the proportion of pixel numbers constituting the actin filaments to those corresponding to the total cell area. Therefore, higher skewness and lower occupancy mean a higher level of actin bundling (Higaki et al., 2010). Relative skewness and occupancy were calculated by dividing the values with those of the abutting lower cell (Fig. 2, B and C). While both skewness and occupancy were almost constant in the TZ, the skewness increased from the second to the last TZ cell to the last TZ cell and from the last TZ cell to the first EDZ cell (Fig. 2C). The occupancy was decreased significantly from the last TZ cell to the first EDZ cell. Both factors became unchanged from the first EDZ cell (Fig. 2C). These results suggest that the second rapid cell elongation is prepared two cells before the first EDZ cell, which undergoes actual cell elongation.

To examine the involvement of actin in root cell elongation, we studied mutants with defects in G-actin production. The Arabidopsis genome encodes three genes for vegetative actin, *ACT2*, *ACT7*, and *ACT8*; all are ubiquitously and highly expressed in the roots (An et al., 1996; Kandasamy et al., 2001). A previous study demonstrated that *ACT2* and *ACT8* cooperatively regulate root hair development, whereas *ACT7* is required for cell division in the PM (Kandasamy et al., 2009). Indeed, the number of PM cells was reduced in the mutant carrying the null *act7-4* allele (hereafter referred to as *act7*) but not in the *act2-1 act8-2* double mutant (hereafter referred as *act2/8*), in which both *ACT2* and *ACT8* are knocked out (Fig. 3B; Kandasamy et al., 2009). On the other hand, both *act2/8* and *act7* mutants had more TZ cells than the wild type, suggesting a delay in the second rapid cell elongation (Fig. 3). Similar results also were obtained using the *act2-5* mutant, with a semidominant negative mutation, and the *act7-6* knockdown mutant (Lanza et al., 2012; Guo et al., 2013; Supplemental Fig. S5). It is noteworthy that cells grow slowly but continuously in the TZ even in the *act* mutants, thereby producing much longer cells at the transition from the TZ to the EDZ in *act7* and *act2/8* mutants as compared with the wild type (Fig. 3A; Supplemental Fig. S6).

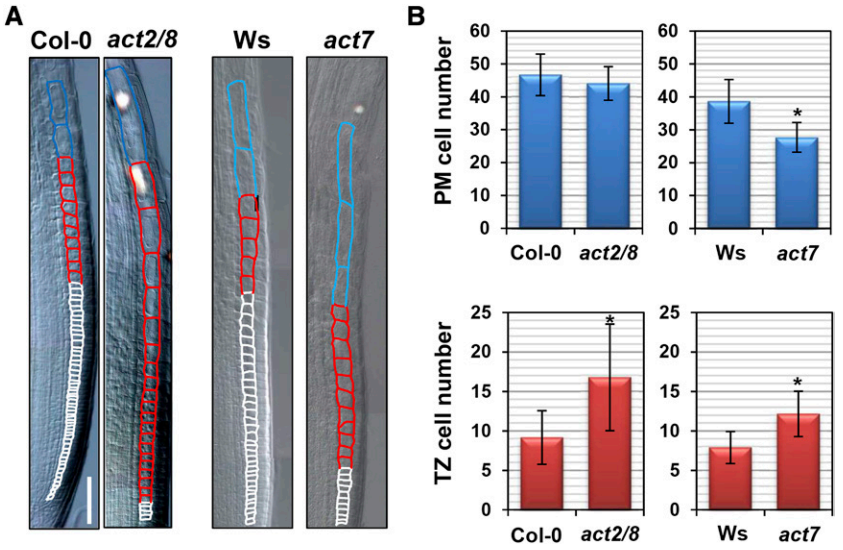

Figure 3. Delay in the second rapid cell elongation in actin mutants. Five-day-old seedlings of wild-type (Columbia-0 [Col-0] and Wassilewskija [Ws]), *act2/8*, and *act7* plants were observed. A, Cortical cells around the TZ. The PM, TZ, and EDZ cells are shown by white, red, and blue outlines, respectively. Bar = 50 μm. B, Number of PM and TZ cells. Data are presented as means ± SD ($n > 20$). Significant differences from the wild type were determined by Student's *t* test: *, $P < 0.001$.

Immunostaining revealed that, in *act7* and *act2/8* mutants, the formation of longitudinally oriented actin bundles was delayed in the longer TZ cells (Supplemental Fig. S6, A and B). To quantify this phenotype, we compared relative skewness and occupancy between the wild type and the *act* mutants. As mentioned above, relative skewness and occupancy increased and decreased, respectively, at the transition from the TZ to the EDZ in the wild-type roots (Fig. 4). By contrast, these metrics displayed less pronounced changes in *act7* and *act2/8* mutants (Fig. 4). These results suggest that the actin rearrangement that occurs at the basal end of the TZ is compromised in the *act7* and *act2/8* mutants, thereby resulting in a delay in the second rapid cell elongation.

The ARP2/3 complex consisting of seven subunits controls the higher order structures of actin filaments during trichome development and lobe formation of pavement cells (Li et al., 2003; Mathur et al., 2003a). Microarray data obtained from the Arabidopsis electronic fluorescent pictograph browser indicated that transcripts of *ARP2* and *ARP3* are accumulated in rapidly elongating root cells (Supplemental Fig. S7A; Winter et al., 2007). Moreover, we found that *arp2* and *arp3* knockout mutants displayed a delay in the second rapid cell elongation and an increase in the number of TZ cells (Supplemental Fig. S7, B and C). Taken together, this and the above results suggest that both G-actin supply by *ACT* genes and actin dynamics regulated by the ARP2/3 complex play important roles in the second rapid cell elongation.

Cytokinins Promote the Second Rapid Cell Elongation

CKs play a central role in promoting the onset of endoreplication that triggers the first rapid cell elongation (Takahashi et al., 2013). Therefore, we asked whether CKs also are involved in the second rapid cell elongation. We first examined the expression of CK-related genes, such as the CK receptors *AHK3* and *AHK4*, and the B-type response regulators *ARR1*, *ARR2*, and *ARR12*. The promoter activity of *AHK4* (Higuchi et al., 2004) was detected in the vasculature (Supplemental Fig. S8A). The translational *GUS-AHK3* fusion gene was highly expressed in the stele but also in other tissues (Supplemental Fig. S8B; Higuchi et al., 2004). The fusion proteins GUS-ARR1, GUS-ARR2, and GUS-ARR12 were accumulated over the area encompassing the TZ and the EDZ (Supplemental Fig. S8B); moreover, the expression of the CK-responsive marker *pARR5:GUS* was not restricted to the vasculature but also observed in other cell types in the root tip (Supplemental Fig. S8C). These expression patterns suggest that CK signaling is activated in various cell types during the second rapid cell elongation.

Next, we examined wild-type roots treated with trans-zeatin (t-zeatin), which has been shown to promote the first rapid cell elongation (Takahashi et al., 2013). Two days of treatment with different concentrations of t-zeatin revealed that 1,000 and 2,000 nM t-zeatin decreased the PM cell number, while 250 nM t-zeatin was sufficient to reduce the TZ cell number (Supplemental Fig. S9A). When we used another CK kinetin for treatments, 20 μM kinetin was required to reduce the PM cell number, whereas 1 or 5 μM kinetin could reduce the TZ cell number (Supplemental Fig. S9B). These results suggest that the second rapid cell elongation that determines the TZ cell number is more sensitive to CKs than the first one. Hereafter, we used 250 nM t-zeatin for treatments, because it affects only the second rapid cell elongation. In the *ahk3/4* double mutant, cell numbers increased in both the PM and the TZ when compared with that of the wild type (Fig. 5). Notably, the reduction in the number of TZ cells upon treatment with 250 nM t-zeatin was suppressed in the *ahk3/4* mutant (Fig. 5). This suggests that CK-induced second rapid cell elongation is mediated by AHK3 and AHK4.

Previous studies demonstrated that CKs promote the first rapid cell elongation through two pathways: the ARR1/12-SHY2 pathway inhibits cell division by suppressing auxin signaling, while the ARR2-CCS52A1

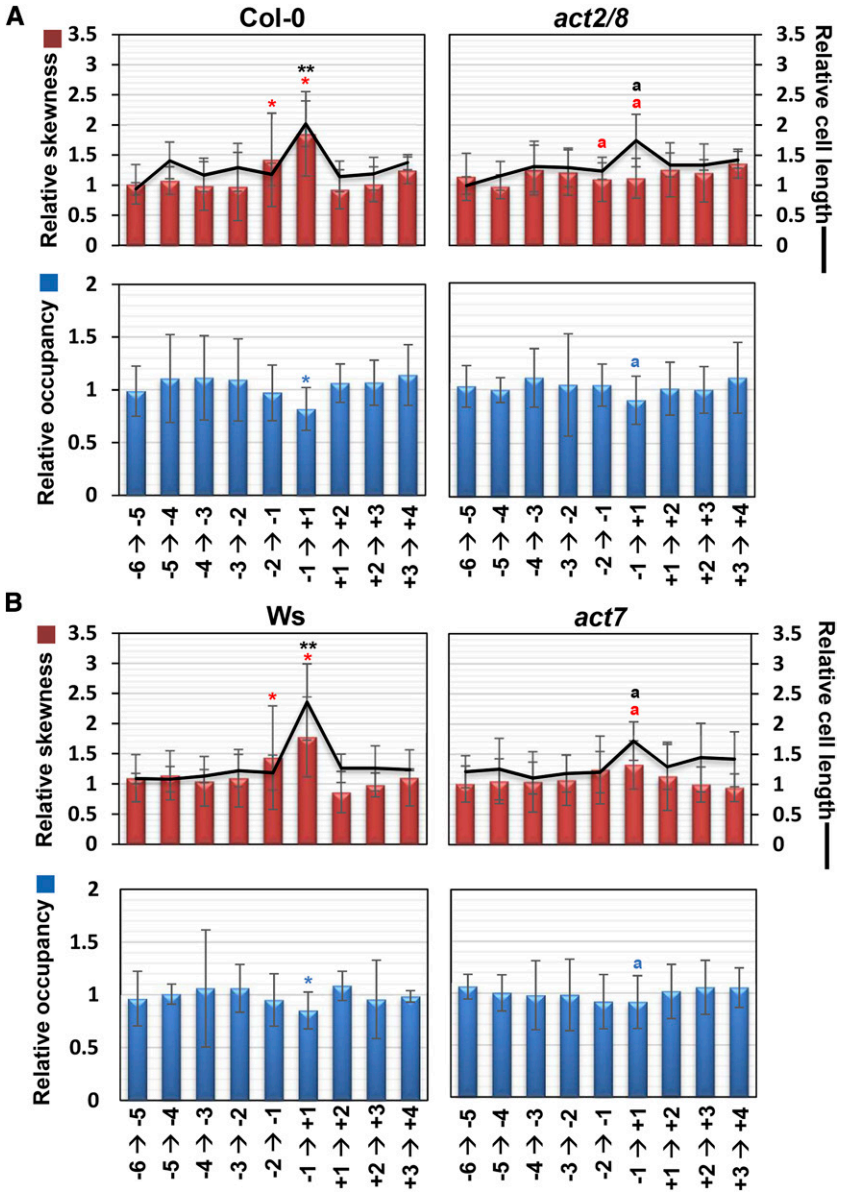

Figure 4. Defects in actin bundling at the boundary between the TZ and the EDZ in actin mutants. Cell length, skewness of intensity distribution (a metric for actin filament bundling), and occupancy of skeletonized pixels (a metric for actin filament density) are indicated as relative values, with that for the adjoining lower cell set to 1. The position of each epidermal cell is represented as shown in Figure 2B. Col-0 (A) and Ws (B) were used as wild-type controls. Data are presented as means ± SD ($n > 15$). Red, blue, and black asterisks or letters indicate significant differences for relative skewness, relative occupancy, and relative cell length, respectively. Asterisks represent significant differences from the adjoining lower cell in the wild type. Bars or lines with different letters differ significantly from the wild type at the same cell position (*P < 0.05, **P < 0.01). Significant differences were determined by Student's *t* test.

pathway promotes the onset of endoreplication (Dello Ioio et al., 2008; Takahashi et al., 2013). Similar to the *ahk3/4* mutant, an increase in the number of TZ cells was observed in the *arr2* mutant when compared with that of the wild type, and the CK-induced decrease was suppressed significantly (Fig. 5). The number of TZ cells in the *arr1/12* double mutant was reduced by t-zeatin treatment, and, in the absence of t-zeatin, this mutant exhibited only a marginal increase in the number of TZ cells when compared with the wild type (Fig. 5). These results suggest that ARR2 functions downstream of AHK3/4 in promoting the second rapid cell elongation. In the knockout mutants of *SHY2* and *CCS52A1*, the number of TZ cells was similar to that in the wild type and was reduced by t-zeatin treatment in a manner similar to that observed in the wild type (Supplemental Fig. S10, A and B). These results suggest that the second rapid cell elongation is promoted by CKs but does not require SHY2 or CCS52A1, which control auxin signaling and the onset of endoreplication, respectively, downstream of CK signaling during the first rapid cell elongation.

Note that the final length of mature EDZ cells is the same between the wild type and the CK-related mutants *ahk3/4*, *arr2*, and *arr1/12* (Supplemental Fig. S11, A and B), suggesting that CK-mediated control of rapid cell elongation does not have an impact on the final cell size in roots.

The AHK3/4-ARR2 Pathway Controls Actin Bundling

To examine whether CKs promote the second rapid cell elongation by controlling actin dynamics, we performed actin immunostaining (Supplemental Fig. S12). The increase and decrease of the skewness and the occupancy, respectively, at the boundary of the TZ

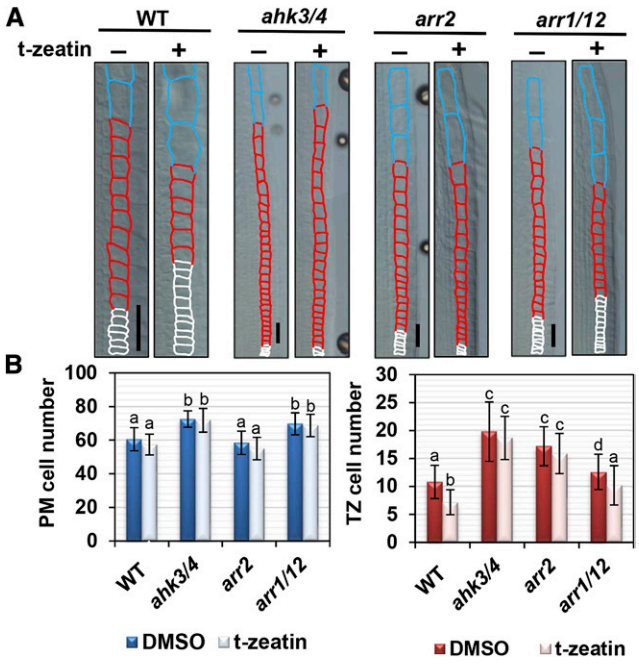

Figure 5. Cytokinins promote the second rapid cell elongation. A, Cortical cells around the TZ in wild-type (WT), *ahk3/4*, *arr2*, and *arr1/12* plants. Five-day-old seedlings were treated with (+) or without (–) 250 nM t-zeatin for 2 d. The PM, TZ, and EDZ cells are shown by white, red, and blue outlines, respectively. Bars = 50 μm. B, Number of PM and TZ cells in wild-type, *ahk3/4*, *arr2*, and *arr1/12* plants. Data are presented as means ± SD ($n > 24$). Bars with different letters differ significantly from each other. Significant differences were determined by Tukey's test ($P < 0.05$). DMSO, Dimethyl sulfoxide.

and the EDZ were enhanced significantly by treatment with 250 nM t-zeatin (Fig. 6). However, in the *ahk3/4* and *arr2* mutants, both values remained unchanged even as cells underwent the second rapid cell elongation and were unaffected by the t-zeatin treatment (Fig. 6). These results suggest that CK signaling is involved in actin bundling, thereby promoting the second rapid cell elongation. We also found that the CK-induced reduction in TZ cell number was suppressed in *act2/8* and *act7* mutants (Supplemental Fig. S13), further supporting the hypothesis that CKs promote the second rapid elongation through controlling actin organization.

DISCUSSION

A previous report indicated that the TZ consists of more cells in CK-related mutants than in the wild type (Lavrekha et al., 2017). However, how CKs control the TZ cell number has not been unraveled thus far. In this study, we demonstrated that Arabidopsis root cells undergo two modes of cell elongation: one occurs at the boundary of the PM and the TZ, and the other occurs between the TZ and the EDZ. We showed that CKs promote the second rapid cell elongation by controlling the rearrangement of actin filaments, thereby restricting the number of TZ cells (Fig. 7). The role of actin in cell elongation has been well studied in leaves. The Arabidopsis mutants with defects in actin organization produce trichomes with a reduced number of branches and distorted shape (Li et al., 2003; Mathur et al., 2003b). Loss-of-function mutations in the components of the ARP2/3 complex cause the mislocalization of diffuse cortical F-actin and inhibit lobe extension in pavement cells, indicating that proper actin organization is essential for the jigsaw-shaped pattern of leaf epidermal cells (Mathur et al., 2003a). In the roots, defects in actin dynamics lead to a variety of phenotypes in root hairs, producing stunted, bulbous, wavy, and branched hairs (Gilliland et al., 2002; Yi et al., 2005), and actin rearrangement was observed in maize (*Zea mays*) root cells (Baluška et al., 1997). Despite these findings, the general involvement of actin in root cell elongation has been largely unknown.

The Arabidopsis genome encodes eight actin genes that are classified into two classes, vegetative and reproductive actins; the former are grouped further into two subclasses, subclass I (*ACT2* and *ACT8*) and subclass II (*ACT7*; Kandasamy et al., 2009). Previous studies demonstrated that each subclass plays partially overlapping but distinct roles in root development; ACT2 and ACT8 are essential for root hair growth, while ACT7 is involved in primary root growth (Kandasamy et al., 2009). To support the functional differentiation, ACT2 and ACT7 have different biochemical properties, for instance, in the binding affinity to profilins, thereby tending to polymerize into the thinner and thicker filaments, respectively (Kijima et al., 2016, 2018). Nevertheless, our results showed that mutants of both subclasses exhibited a dramatic delay in the second rapid cell elongation, indicating that vegetative actins are crucial for elongating TZ cells irrespective of the subclass.

Previous reports demonstrated that auxin promotes actin bundling (Li et al., 2014; Zhu and Geisler, 2015; Scheuring et al., 2016), while a high concentration of auxin unbundles actin filaments in Arabidopsis roots (Lanza et al., 2012; Zhu and Geisler, 2015), suggesting a concentration-dependent effect of auxin on actin dynamics. On the other hand, the involvement of CK in actin organization has been poorly understood. Kushwah et al. (2011) reported that, when Arabidopsis roots were treated with the synthetic CK 6-benzylaminopurine, tightly meshed actin filaments were formed, suggesting a negative effect on actin bundling. This result is not consistent with our data for CK-induced actin bundling. One possible explanation for this inconsistency is that the sensitivity to CK differs depending on the extent of cell differentiation. Although Kushwah et al. (2011) did not describe the cell type used for observation, our results show that 250 nM t-zeatin promoted the second rapid cell elongation but not the first one, suggesting that CK effects are probably

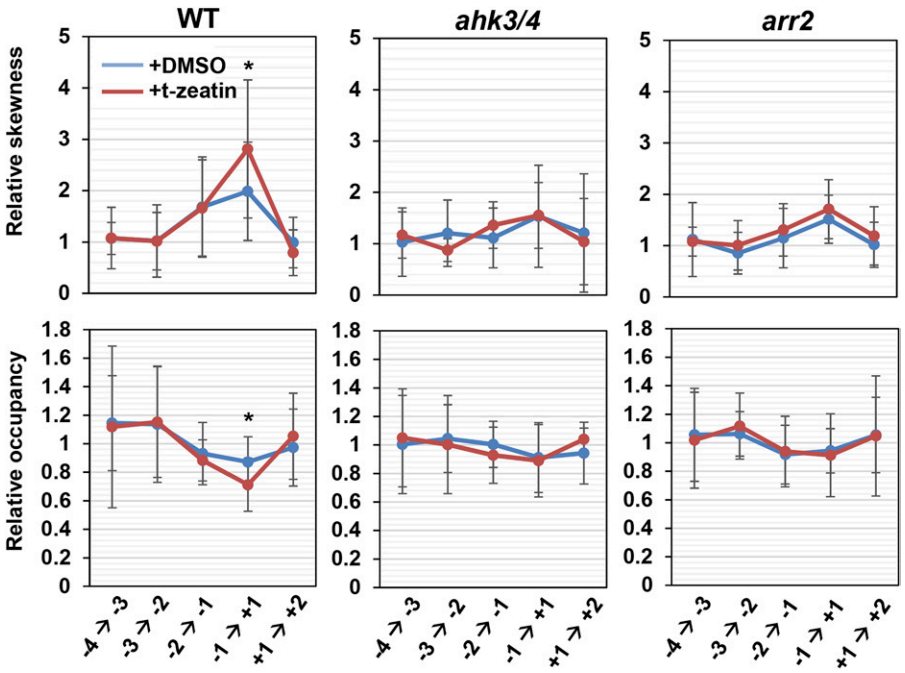

Figure 6. Cytokinins promote actin bundling at the boundary between the TZ and the EDZ. Skewness of intensity distribution (a metric for actin filament bundling) and occupancy of skeletonized pixels (a metric for actin filament density) are indicated as relative values, with that for the adjoining lower cell set to a value of 1. The position of each epidermal cell is represented as shown in Figure 2B. Col-0 was used as the wild-type (WT) control. Data are presented as means ± SD ($n > 15$). Significant differences from the dimethyl sulfoxide (DMSO)-treated control at the same cell position were determined by Student's *t* test: *, $P < 0.05$.

different depending on the cell type and/or levels of cell differentiation. Kushwah et al. (2011) used 1 μM 6-benzylaminopurine for treatments; therefore, it is also possible that CKs control actin bundling in a concentration-dependent manner, as described above for auxin.

Our results suggested that AHK3/4 and ARR2 promote the second rapid cell elongation. However, the downstream pathway remains unknown. While no actin-related gene has been reported as a direct target of B-type ARRs (Taniguchi et al., 2007; Zubo et al., 2017), some genes respond to CK treatment; for example, *ACTIN DEPOLYMERIZING FACTOR9* (*ADF9*) encoding a member of ADF/cofilin, which modulates actin filament turnover, is up-regulated by CKs in roots (Burgos-Rivera et al., 2008). Rho-of-plant (ROP) signaling is enhanced by CKs, thereby controlling actin organization and the shape of leaf pavement cells (Li et al., 2013). Further studies will reveal how CK signaling regulates actin modulators and/or factors related to ROP signaling and promotes the second rapid cell elongation. Our results indicated that SHY2, a member of the Aux/IAA family, is not involved in the second rapid cell elongation (Fig. 7). We cannot yet deny the possibility of other Aux/IAA proteins functioning in actin bundling because the expression of some Aux/IAA family members was altered upon t-zeatin treatment in the roots (Jones et al., 2010). It is also possible that CKs control actin dynamics through another hormonal signaling pathway. Previous studies indicated that *ARR2* promotes stomatal closure in collaboration with *ETHYLENE-INSENSITIVE2* (*EIN2*), a central regulator of ethylene signaling (Desikan et al., 2006), and that the *ein2* mutant is resistant to CKs in terms of root growth inhibition. These observations raise the possibility that ethylene signaling could mediate CK-induced actin bundling during the second rapid cell elongation.

Previous studies indicated that the TZ is the site of the response to environmental cues and the control of root growth and that CKs function in sensing environmental signals such as drought stress and gravity stimulations (Aloni et al., 2004; Nishiyama et al., 2011). For instance, the stress hormone abscisic acid reduces the expression levels of B-type ARRs, *ARR1*, *ARR10*, and *ARR12*, and enlarges the size of the TZ (Zhang et al., 2010; Nguyen et al., 2016). These findings suggest that environmental factors regulate CK signaling, thereby modulating the onset of the second rapid cell elongation and the TZ size. Identification of the upstream signaling pathways that trigger CK-induced actin bundling will reveal the mechanism associated with fine-tuning root growth under changing environmental conditions.

MATERIALS AND METHODS

Plant Materials and Growth Conditions

Arabidopsis (*Arabidopsis thaliana* ecotypes Col-0 and Ws) was grown vertically on Murashige and Skoog (MS) plates (1× MS salts, 0.5 g L^{-1} MES, 1× MS vitamin solution, 1% (w/v) Suc, and 0.4% (w/v) phytagel [pH 6.3]) under continuous light conditions at 22°C. Mutant plants *act7-4*, *act7-6*, *act2-5*, *arr2* (*arr2-4*), *arr1/12* (*arr1-3 arr12-1*), *ahk3/4* (*ahk3-1 ahk4-1*), *ccs52a1* (*ccs52a1-1*), *shy2-31*, *arp2* (*wrm-T1*), and *arp3* (*dis1-2*) and the transgenic lines *pVAM3-GFP::VAM3*, *pAHK4-GUS*, *pAHK3-AHK3::GUS*, *pARR5-GUS*, *pARR1-ARR1::GUS*, and *pARR2-ARR2::GUS* were described previously (D'Agostino et al., 2000; Le et al., 2003; Higuchi et al., 2004; Mason et al., 2005; Larson-Rabin et al., 2009; Uemura et al., 2010; Kim et al., 2012; Lanza et al., 2012; Guo et al., 2013; Takahashi et al., 2013). The mutant *act2/8* (*act2-1 act8-2*) was a gift from Dr. Abidur Rahman. Chemicals used in this study are BCECF-AM (Life Technologies), t-zeatin, kinetin (Nacalai Tesque), and colchicine (Wako).

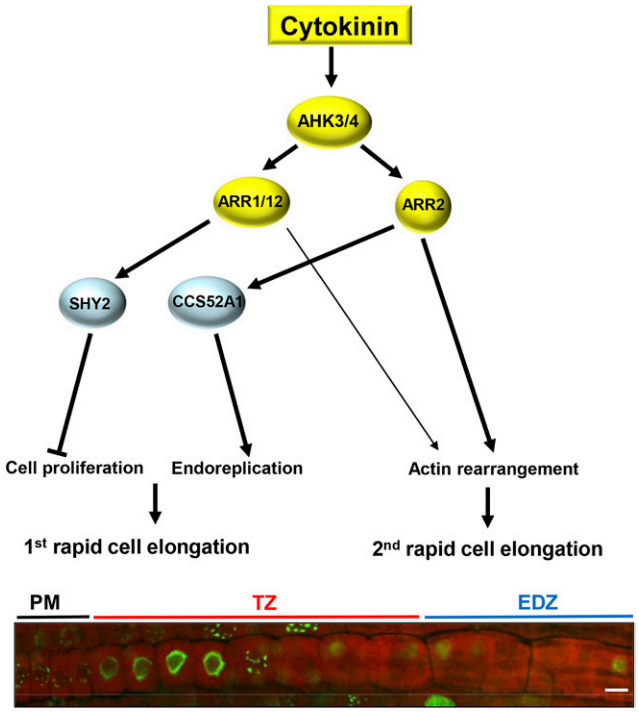

Figure 7. Model for CK-mediated control of root cell elongation in Arabidopsis. The CK signal mediated through the receptors AHK3 and AHK4 and the B-type response regulators ARR1, ARR2, and ARR12 inhibits cell proliferation and promotes endoreplication and actin rearrangement. As a result, two modes of rapid cell elongation occur at the boundaries between the PM and the TZ and between the TZ and the EDZ. *SHY2*, encoding one of the Aux/IAA family members, is up-regulated by ARR1/12, while ARR2 induces the expression of *CCS52A1*, thereby activating the APC/C and triggering the onset of endoreplication. Bar = 10 μm.

Plasmid Construction

To create *pARR1-ARR1*::*GUS*, *pARR2-ARR2*::*GUS*, and *pARR12–ARR12*::*GUS*, the genomic fragments of *ARR1*, *ARR2*, and *ARR12*, from 2,000, 2,000, and 1,997 bp, respectively, upstream of the start codon to 1 bp before the stop codon, were amplified by PCR using the following primers: 5′-AAAAAGCAGGCTGACAACGATAGATGGAGAGG-3′ and 5′-AGAAAGCTGGGTAAACCGGAATGTTATCGATGG-3′ for *ARR1*, 5′-AAAAAGCAGGCTGGATCCACGTATCAAGGGTC-3′ and 5′-AGAAAGCTGGGTAGACCTGGATATTATCGATGG-3′ for *ARR2*, and 5′-AAAAAGCAGGCTGTCAGTTTACTATCTTTTGTACC-3′ and 5′-AGAAAGCTGGGTATATGCATGTTCTGAGTGAAC-3′ for *ARR12*. The resultant fragments were cloned into the Gateway entry vector pDONR221 (Invitrogen). A recombination reaction was conducted between the entry clone and the Gateway destination vector pGWB3 (Nakagawa et al., 2007) using LR clonase (Invitrogen) to generate the *GUS* fusion genes.

Microscopy

For measurement of the PM and TZ cell number, roots were cleared with a clearing solution (8 g of chloral hydrate, 1 mL of glycerol, and 2 mL of water) as described by Takahashi et al. (2013). Immunostained roots and those stained with PI, EdU, or BCECF-AM were observed with a confocal laser scanning microscope (Olympus; FluoView FV1000).

EdU Staining

EdU staining was performed with the Click-iT EdU Alexa Fluor 488 Imaging Kit (Thermo Fisher Scientific) according to the manufacturer's instructions. In brief, seedlings were immersed in liquid MS medium containing 20 μM EdU for 30 min and fixed in phosphate-buffered saline (PBS; 130 mM NaCl, 5.1 mM Na_2HPO_4, and 1.6 mM KH_2PO_4, pH 7.4) containing 4% (w/v) formaldehyde and 0.1% Triton X-100 for 30 min. After washing twice with PBS containing 3% bovine serum albumin, samples were incubated in the Click-iT reaction cocktail for 30 min in the dark. The reaction cocktail was then removed, and samples were washed three times with PBS.

Cell and Vacuole Size Measurements

BCECF-AM staining was performed as described previously (Scheuring et al., 2015). In brief, seedlings were immersed in liquid MS medium containing 10 nM BCECF-AM for 2 h and then washed with liquid MS medium. Roots were mounted on a glass slide under a coverslip in distilled water containing 10 μg mL^{-1} PI. Atrichoblast cells of the root epidermis were observed with a confocal microscope with excitation wavelengths at 488 and 568 nm for BCECF-AM and PI, respectively. Using PI-labeled cell wall images, cell regions were segmented automatically by an ImageJ plug-in, Morphological Segmentation (tolerance = 35–50; Legland et al., 2016). BCECF-labeled vacuole regions were segmented by Otsu thresholding. Based on these segmented images, cell and vacuole volumes were measured by an ImageJ plug-in, 3D Roi Manager (Ollion et al., 2013).

GUS Staining

Roots were fixed in 90% (v/v) acetone for 15 min on ice, washed with GUS buffer [100 mM Na_2HPO_4 (pH 7), 5 mM $K_3Fe(CN)_6$, and 5 mM $K_4Fe(CN)_6$], and immersed in the same buffer containing 0.5 mg mL^{-1} 5-bromo-4-chloro-3-indolyl-β-D-glucuronide. The samples were then degassed for 15 min and incubated at 37°C.

Immunostaining

To immunostain actin and MTs, primary root sections were placed in a fixing solution containing 1.5% formaldehyde and 0.5% glutaraldehyde. Immunostaining was conducted as described by Abe and Hashimoto (2005). Monoclonal anti-actin antibody (Sigma; A0605) and anti-tubulin antibody (Abcam; ab6160) were used as primary antibodies, while anti-mouse IgG-fluorescein isothiocyanate antibody (Sigma; F0257) and goat anti-rat IgG cross-adsorbed secondary antibody Alexa Fluor 568 (Thermo Fisher Scientific; A-11077) were used as secondary antibodies. Atrichoblast cells of the root epidermis were observed with a confocal microscope with excitation wavelength at 488 or 568 nm.

Quantification of MT and Actin Filament Organization

Immunostained images were skeletonized using ImageJ plug-ins: Lpx-LineExtract, which is invoked by Lpx_Filter2d plug-ins (filter = lineFilters, linemode = lineExtract) in the LPixel ImageJ plugins package (available for free at https://lpixel.net/services/research/lpixel-imagej-plugins/). The parameters were as follows: giwsIter = 5, mdnmsLen = 15, pickup = above, shaveLen = 20, and delLen = 20. The skeletonized images were masked with a 5-μm-square region at the center of the cell. The masked skeletonized images were used to measure the skewness of the intensity distribution of the skeletonized pixels and the occupancy of the skeletonized pixels as metrics for actin filament bundling and density, respectively (Higaki et al., 2010). The masked skeletonized images of MTs were used to measure mean angles against the major cell axis, parallelness, and occupancy as metrics for MT orientation, variation of the orientation, and density, respectively (Kimata et al., 2016; Higaki, 2017). Measurements were performed using ImageJ plug-ins: Lpx-LineFeature, which is invoked by Lpx_Filter2d plug-ins (filter = lineFilters, linemode = lineFeature) in the LPixel ImageJ plugins package.

Accession Numbers

Sequence data from this article can be found in the Arabidopsis Genome Initiative database under the following accession numbers: *ACT2* (AT3G18780), *ACT7* (AT5G09810), *ACT8* (AT1G49240), *ARP2* (AT3G27000), *ARP3* (AT1G13180), *AHK3* (AT1G27320), *AHK4* (AT2G01830), *ARR5* (AT3G48100), *ARR1* (AT3G16857), *ARR2* (AT4G16110), *ARR12* (AT2G25180), *SHY2* (AT1G04240), and *CCS52A1* (AT4G22910).

Supplemental Data

The following supplemental materials are available.

Supplemental Figure S1. Cell length over the distinct zones of roots.

Supplemental Figure S2. Cell elongation in the root epidermis.

Supplemental Figure S3. Vacuoles in the root epidermis.

Supplemental Figure S4. MTs in the root epidermis.

Supplemental Figure S5. Delay in the second rapid cell elongation in *act2-5* and *act7-6* mutants.

Supplemental Figure S6. Actin organization in the root epidermis of actin mutants.

Supplemental Figure S7. PM and TZ cell numbers in *arp2* and *arp3* mutants.

Supplemental Figure S8. Expression pattern of genes related to CK signaling in roots.

Supplemental Figure S9. Effects of CKs on the PM and TZ cell numbers.

Supplemental Figure S10. PM and TZ cell numbers in *ahk3/4*, *shy2-31*, and *ccs52a1* mutants.

Supplemental Figure S11. Mature cortex cells of 5-d-old wild-type, *ahk3/4*, *arr2*, and *arr1/12* roots.

Supplemental Figure S12. Actin organization in the root epidermis of *ahk3/4* and *arr2* mutants.

Supplemental Figure S13. Suppression of CK-induced reduction in TZ cell number in *act2/8* and *act7* mutants.

ACKNOWLEDGMENTS

We thank Dr. Abidur Rahman for the gift of the *act7-4* and *act2-1 act8-2* mutants and Dr. Markus Grebe and Dr. Antonio Leyva for providing the *act7-6* and *act2-5* mutants, respectively.

Received May 8, 2018; accepted August 27, 2018; published September 5, 2018.

LITERATURE CITED

Abe T, Hashimoto T (2005) Altered microtubule dynamics by expression of modified α-tubulin protein causes right-handed helical growth in transgenic Arabidopsis plants. Plant J **43**: 191–204

Adachi S, Minamisawa K, Okushima Y, Inagaki S, Yoshiyama K, Kondou Y, Kaminuma E, Kawashima M, Toyoda T, Matsui M, (2011) Programmed induction of endoreduplication by DNA double-strand breaks in Arabidopsis. Proc Natl Acad Sci USA **108**: 10004–10009

Aloni R, Langhans M, Aloni E, Ullrich CI (2004) Role of cytokinin in the regulation of root gravitropism. Planta **220**: 177–182

An YQ, McDowell JM, Huang S, McKinney EC, Chambliss S, Meagher RB (1996) Strong, constitutive expression of the Arabidopsis ACT2/ACT8 actin subclass in vegetative tissues. Plant J **10**: 107–121

Baluška F, Vitha S, Barlow PW, Volkmann D (1997) Rearrangements of F-actin arrays in growing cells of intact maize root apex tissues: a major developmental switch occurs in the postmitotic transition region. Eur J Cell Biol **72**: 113–121

Baluška F, Mancuso S, Volkmann D, Barlow PW (2010) Root apex transition zone: a signalling-response nexus in the root. Trends Plant Sci **15**: 402–408

Baskin TI, Beemster GT, Judy-March JE, Marga F (2004) Disorganization of cortical microtubules stimulates tangential expansion and reduces the uniformity of cellulose microfibril alignment among cells in the root of Arabidopsis. Plant Physiol **135**: 2279–2290

Blilou I, Xu J, Wildwater M, Willemsen V, Paponov I, Friml J, Heidstra R, Aida M, Palme K, Scheres B (2005) The PIN auxin efflux facilitator network controls growth and patterning in Arabidopsis roots. Nature **433**: 39–44

Braidwood L, Breuer C, Sugimoto K (2014) My body is a cage: mechanisms and modulation of plant cell growth. New Phytol **201**: 388–402

Burgos-Rivera B, Ruzicka DR, Deal RB, McKinney EC, King-Reid L, Meagher RB (2008) ACTIN DEPOLYMERIZING FACTOR9 controls development and gene expression in Arabidopsis. Plant Mol Biol **68**: 619–632

Casamitjana-Martínez E, Hofhuis HF, Xu J, Liu CM, Heidstra R, Scheres B (2003) Root-specific CLE19 overexpression and the sol1/2 suppressors implicate a CLV-like pathway in the control of Arabidopsis root meristem maintenance. Curr Biol **13**: 1435–1441

Cebolla A, Vinardell JM, Kiss E, Oláh B, Roudier F, Kondorosi A, Kondorosi E (1999) The mitotic inhibitor ccs52 is required for endoreduplication and ploidy-dependent cell enlargement in plants. EMBO J **18**: 4476–4484

D'Agostino IB, Deruère J, Kieber JJ (2000) Characterization of the response of the Arabidopsis response regulator gene family to cytokinin. Plant Physiol **124**: 1706–1717

Dello Ioio R, Linhares FS, Scacchi E, Casamitjana-Martinez E, Heidstra R, Costantino P, Sabatini S (2007) Cytokinins determine Arabidopsis root-meristem size by controlling cell differentiation. Curr Biol **17**: 678–682

Dello Ioio R, Nakamura K, Moubayidin L, Perilli S, Taniguchi M, Morita MT, Aoyama T, Costantino P, Sabatini S (2008) A genetic framework for the control of cell division and differentiation in the root meristem. Science **322**: 1380–1384

Desikan R, Last K, Harrett-Williams R, Tagliavia C, Harter K, Hooley R, Hancock JT, Neill SJ (2006) Ethylene-induced stomatal closure in Arabidopsis occurs via AtrbohF-mediated hydrogen peroxide synthesis. Plant J **47**: 907–916

Doerner P, Jørgensen JE, You R, Steppuhn J, Lamb C (1996) Control of root growth and development by cyclin expression. Nature **380**: 520–523

Dolan L, Davies J (2004) Cell expansion in roots. Curr Opin Plant Biol **7**: 33–39

Fu Y (2015) The cytoskeleton in the pollen tube. Curr Opin Plant Biol **28**: 111–119

Fu Y, Li H, Yang Z (2002) The ROP2 GTPase controls the formation of cortical fine F-actin and the early phase of directional cell expansion during *Arabidopsis* organogenesis. Plant Cell **14**: 777–794

Fu Y, Gu Y, Zheng Z, Wasteneys G, Yang Z (2005) Arabidopsis interdigitating cell growth requires two antagonistic pathways with opposing action on cell morphogenesis. Cell **120**: 687–700

Gilliland LU, Kandasamy MK, Pawloski LC, Meagher RB (2002) Both vegetative and reproductive actin isovariants complement the stunted root hair phenotype of the Arabidopsis act2-1 mutation. Plant Physiol **130**: 2199–2209

Guo B, Chen Y, Zhang G, Xing J, Hu Z, Feng W, Yao Y, Peng H, Du J, Zhang Y, (2013) Comparative proteomic analysis of embryos between a maize hybrid and its parental lines during early stages of seed germination. PLoS ONE **8**: e65867

Haruta M, Sabat G, Stecker K, Minkoff BB, Sussman MR (2014) A peptide hormone and its receptor protein kinase regulate plant cell expansion. Science **343**: 408–411

Hayashi K, Hasegawa J, Matsunaga S (2013) The boundary of the meristematic and elongation zones in roots: endoreduplication precedes rapid cell expansion. Sci Rep **3**: 2723

Higaki T (2017) Quantitative evaluation of cytoskeletal organizations by microscopic image analysis. Plant Morphology **29**: 15–21

Higaki T, Kutsuna N, Sano T, Kondo N, Hasezawa S (2010) Quantification and cluster analysis of actin cytoskeletal structures in plant cells: role of actin bundling in stomatal movement during diurnal cycles in Arabidopsis guard cells. Plant J **61**: 156–165

Higuchi M, Pischke MS, Mähönen AP, Miyawaki K, Hashimoto Y, Seki M, Kobayashi M, Shinozaki K, Kato T, Tabata S, (2004) In planta functions of the Arabidopsis cytokinin receptor family. Proc Natl Acad Sci USA **101**: 8821–8826

Hwang I, Sheen J (2001) Two-component circuitry in Arabidopsis cytokinin signal transduction. Nature **413**: 383–389

Inoue T, Higuchi M, Hashimoto Y, Seki M, Kobayashi M, Kato T, Tabata S, Shinozaki K, Kakimoto T (2001) Identification of CRE1 as a cytokinin receptor from Arabidopsis. Nature **409**: 1060–1063

Jones B, Gunnerås SA, Petersson SV, Tarkowski P, Graham N, May S, Dolezal K, Sandberg G, Ljung K (2010) Cytokinin regulation of auxin synthesis in *Arabidopsis* involves a homeostatic feedback loop regulated via auxin and cytokinin signal transduction. Plant Cell **22**: 2956–2969

Kandasamy MK, Gilliland LU, McKinney EC, Meagher RB (2001) One plant actin isovariant, ACT7, is induced by auxin and required for normal callus formation. Plant Cell **13**: 1541–1554

Kandasamy MK, McKinney EC, Meagher RB (2009) A single vegetative actin isovariant overexpressed under the control of multiple regulatory sequences is sufficient for normal *Arabidopsis* development. Plant Cell **21**: 701–718

Kijima ST, Hirose K, Kong SG, Wada M, Uyeda TQP (2016) Distinct biochemical properties of Arabidopsis thaliana actin isoforms. Plant Cell Physiol **57**: 46–56

Kijima ST, Staiger CJ, Katoh K, Nagasaki A, Ito K, Uyeda TQP (2018) Arabidopsis vegetative actin isoforms, AtACT2 and AtACT7, generate distinct filament arrays in living plant cells. Sci Rep **8**: 4381

Kim K, Ryu H, Cho YH, Scacchi E, Sabatini S, Hwang I (2012) Cytokinin-facilitated proteolysis of ARABIDOPSIS RESPONSE REGULATOR 2 attenuates signaling output in two-component circuitry. Plant J **69**: 934–945

Kimata Y, Higaki T, Kawashima T, Kurihara D, Sato Y, Yamada T, Hasezawa S, Berger F, Higashiyama T, Ueda M (2016) Cytoskeleton dynamics control the first asymmetric cell division in Arabidopsis zygote. Proc Natl Acad Sci USA **113**: 14157–14162

Kushwah S, Jones AM, Laxmi A (2011) Cytokinin interplay with ethylene, auxin, and glucose signaling controls Arabidopsis seedling root directional growth. Plant Physiol **156**: 1851–1866

Lanza M, Garcia-Ponce B, Castrillo G, Catarecha P, Sauer M, Rodriguez-Serrano M, Páez-García A, Sánchez-Bermejo E, Mohan TC, Leo del Puerto Y, (2012) Role of actin cytoskeleton in brassinosteroid signaling and in its integration with the auxin response in plants. Dev Cell **22**: 1275–1285

Larson-Rabin Z, Li Z, Masson PH, Day CD (2009) FZR2/CCS52A1 expression is a determinant of endoreduplication and cell expansion in Arabidopsis. Plant Physiol **149**: 874–884

Lavrekha VV, Pasternak T, Ivanov VB, Palme K, Mironova VV (2017) 3D analysis of mitosis distribution highlights the longitudinal zonation and diarch symmetry in proliferation activity of the Arabidopsis thaliana root meristem. Plant J **92**: 834–845

Le J, El-Assal SD, Basu D, Saad ME, Szymanski DB (2003) Requirements for Arabidopsis ATARP2 and ATARP3 during epidermal development. Curr Biol **13**: 1341–1347

Le J, Vandenbussche F, De Cnodder T, Van Der Straeten D, Verbelen JP (2005) Cell elongation and microtubule behavior in the Arabidopsis hypocotyl: responses to ethylene and auxin. J Plant Growth Regul **24**: 166–178

Lee HO, Davidson JM, Duronio RJ (2009) Endoreplication: polyploidy with purpose. Genes Dev **23**: 2461–2477

Legland D, Arganda-Carreras I, Andrey P (2016) MorphoLibJ: integrated library and plugins for mathematical morphology with ImageJ. Bioinformatics **32**: 3532–3534

Li G, Liang W, Zhang X, Ren H, Hu J, Bennett MJ, Zhang D (2014) Rice actin-binding protein RMD is a key link in the auxin-actin regulatory loop that controls cell growth. Proc Natl Acad Sci USA **111**: 10377–10382

Li H, Xu T, Lin D, Wen M, Xie M, Duclercq J, Bielach A, Kim J, Reddy GV, Zuo J, (2013) Cytokinin signaling regulates pavement cell morphogenesis in Arabidopsis. Cell Res **23**: 290–299

Li S, Blanchoin L, Yang Z, Lord EM (2003) The putative Arabidopsis arp2/3 complex controls leaf cell morphogenesis. Plant Physiol **132**: 2034–2044

Mason MG, Mathews DE, Argyros DA, Maxwell BB, Kieber JJ, Alonso JM, Ecker JR, Schaller GE (2005) Multiple type-B response regulators mediate cytokinin signal transduction in *Arabidopsis*. Plant Cell **17**: 3007–3018

Mathur J, Spielhofer P, Kost B, Chua N (1999) The actin cytoskeleton is required to elaborate and maintain spatial patterning during trichome cell morphogenesis in Arabidopsis thaliana. Development **126**: 5559–5568

Mathur J, Mathur N, Kernebeck B, Hülskamp M (2003a) Mutations in actin-related proteins 2 and 3 affect cell shape development in *Arabidopsis*. Plant Cell **15**: 1632–1645

Mathur J, Mathur N, Kirik V, Kernebeck B, Srinivas BP, Hülskamp M (2003b) Arabidopsis CROOKED encodes for the smallest subunit of the ARP2/3 complex and controls cell shape by region specific fine F-actin formation. Development **130**: 3137–3146

Nakagawa T, Kurose T, Hino T, Tanaka K, Kawamukai M, Niwa Y, Toyooka K, Matsuoka K, Jinbo T, Kimura T (2007) Development of series of Gateway binary vectors, pGWBs, for realizing efficient construction of fusion genes for plant transformation. J Biosci Bioeng **104**: 34–41

Nguyen KH, Ha CV, Nishiyama R, Watanabe Y, Leyva-González MA, Fujita Y, Tran UT, Li W, Tanaka M, Seki M, (2016) *Arabidopsis* type B cytokinin response regulators ARR1, ARR10, and ARR12 negatively regulate plant responses to drought. Proc Natl Acad Sci USA **113**: 3090–3095

Nishiyama R, Watanabe Y, Fujita Y, Le DT, Kojima M, Werner T, Vankova R, Yamaguchi-Shinozaki K, Shinozaki K, Kakimoto T, (2011) Analysis of cytokinin mutants and regulation of cytokinin metabolic genes reveals important regulatory roles of cytokinins in drought, salt and abscisic acid responses, and abscisic acid biosynthesis. Plant Cell **23**: 2169–2183

Nowack MK, Harashima H, Dissmeyer N, Zhao X, Bouyer D, Weimer AK, De Winter F, Yang F, Schnittger A (2012) Genetic framework of cyclin-dependent kinase function in Arabidopsis. Dev Cell **22**: 1030–1040

Ollion J, Cochennec J, Loll F, Escudé C, Boudier T (2013) TANGO: a generic tool for high-throughput 3D image analysis for studying nuclear organization. Bioinformatics **29**: 1840–1841

Otero S, Desvoyes B, Peiró R, Gutierrez C (2016) Histone H3 dynamics reveal domains with distinct proliferation potential in the *Arabidopsis* root. Plant Cell **28**: 1361–1371

Pei W, Du F, Zhang Y, He T, Ren H (2012) Control of the actin cytoskeleton in root hair development. Plant Sci **187**: 10–18

Rojo E, Gillmor CS, Kovaleva V, Somerville CR, Raikhel NV (2001) VACUOLELESS1 is an essential gene required for vacuole formation and morphogenesis in Arabidopsis. Dev Cell **1**: 303–310

Sakai H, Honma T, Aoyama T, Sato S, Kato T, Tabata S, Oka A (2001) ARR1, a transcription factor for genes immediately responsive to cytokinins. Science **294**: 1519–1521

Scheuring D, Schöller M, Kleine-Vehn J, Löfke C (2015) Vacuolar staining methods in plant cells. Methods Mol Biol **1242**: 83–92

Scheuring D, Löfke C, Krüger F, Kittelmann M, Eisa A, Hughes L, Smith RS, Hawes C, Schumacher K, Kleine-Vehn J (2016) Actin-dependent vacuolar occupancy of the cell determines auxin-induced growth repression. Proc Natl Acad Sci USA **113**: 452–457

Skoufias DA, Wilson L (1992) Mechanism of inhibition of microtubule polymerization by colchicine: inhibitory potencies of unliganded colchicine and tubulin-colchicine complexes. Biochemistry **31**: 738–746

Smith LG, Oppenheimer DG (2005) Spatial control of cell expansion by the plant cytoskeleton. Annu Rev Cell Dev Biol **21**: 271–295

Szymanski DB, Marks MD, Wick SM (1999) Organized F-actin is essential for normal trichome morphogenesis in *Arabidopsis*. Plant Cell **11**: 2331–2347

Takahashi N, Kajihara T, Okamura C, Kim Y, Katagiri Y, Okushima Y, Matsunaga S, Hwang I, Umeda M (2013) Cytokinins control endocycle onset by promoting the expression of an APC/C activator in Arabidopsis roots. Curr Biol **23**: 1812–1817

Takatsuka H, Umeda M (2014) Hormonal control of cell division and elongation along differentiation trajectories in roots. J Exp Bot **65**: 2633–2643

Takatsuka H, Umeda M (2015) Epigenetic control of cell division and cell differentiation in the root apex. Front Plant Sci **6**: 1178

Takatsuka H, Ohno R, Umeda M (2009) The Arabidopsis cyclin-dependent kinase-activating kinase CDKF;1 is a major regulator of cell proliferation and cell expansion but is dispensable for CDKA activation. Plant J **59**: 475–487

Taniguchi M, Sasaki N, Tsuge T, Aoyama T, Oka A (2007) ARR1 directly activates cytokinin response genes that encode proteins with diverse regulatory functions. Plant Cell Physiol **48**: 263–277

To JPC, Kieber JJ (2008) Cytokinin signaling: two-components and more. Trends Plant Sci **13**: 85–92

To JPC, Haberer G, Ferreira FJ, Deruère J, Mason MG, Schaller GE, Alonso JM, Ecker JR, Kieber JJ (2004) Type-A *Arabidopsis* response regulators are partially redundant negative regulators of cytokinin signaling. Plant Cell **16**: 658–671

Uemura T, Morita MT, Ebine K, Okatani Y, Yano D, Saito C, Ueda T, Nakano A (2010) Vacuolar/pre-vacuolar compartment Qa-SNAREs VAM3/SYP22 and PEP12/SYP21 have interchangeable functions in Arabidopsis. Plant J **64**: 864–873

Verbelen JP, De Cnodder T, Le J, Vissenberg K, Baluška F (2006) The root apex of Arabidopsis thaliana consists of four distinct zones of growth activities: meristematic zone, transition zone, fast elongation zone and growth terminating zone. Plant Signal Behav **1**: 296–304

Winter D, Vinegar B, Nahal H, Ammar R, Wilson GV, Provart NJ (2007) An "Electronic Fluorescent Pictograph" browser for exploring and analyzing large-scale biological data sets. PLoS ONE **2**: e718

Yi K, Guo C, Chen D, Zhao B, Yang B, Ren H (2005) Cloning and functional characterization of a formin-like protein (AtFH8) from Arabidopsis. Plant Physiol **138**: 1071–1082

Zhang H, Han W, De Smet I, Talboys P, Loya R, Hassan A, Rong H, Jürgens G, Knox JP, Wang MH (2010) ABA promotes quiescence of the quiescent centre and suppresses stem cell differentiation in the Arabidopsis primary root meristem. Plant J **64**: 764–774

Zhao Y, Zhao S, Mao T, Qu X, Cao W, Zhang L, Zhang W, He L, Li S, Ren S, (2011) The plant-specific actin binding protein SCAB1 stabilizes actin filaments and regulates stomatal movement in *Arabidopsis*. Plant Cell **23**: 2314–2330

Zhu J, Geisler M (2015) Keeping it all together: auxin-actin crosstalk in plant development. J Exp Bot **66**: 4983–4998

Zubo YO, Blakley IC, Yamburenko MV, Worthen JM, Street IH, Franco-Zorrilla JM, Zhang W, Hill K, Raines T, Solano R, (2017) Cytokinin induces genome-wide binding of the type-B response regulator ARR10 to regulate growth and development in *Arabidopsis*. Proc Natl Acad Sci USA **114**: E5995–E6004